J|A|C|S COMMUNICATIONS

Published on Web 04/02/2009

Insight into Environmental Effects on Bonding and Redox Properties of [4Fe-4S] Clusters in Proteins

Shuqiang Niu and Toshiko Ichiye*

Department of Chemistry, Georgetown University, Washington, D.C. 20057-1227

Received January 19, 2009; E-mail: ti9@georgetown.edu

A classical question about oxidation−reduction potentials in proteins is why the [4Fe−4S] clusters in the high potential iron−sulfur proteins (HiPIPs) have a 1−/2− reduction at 100 to 450 mV vs NHE, while the ferredoxins (Fds) have a 2−/3− reduction at −100 to −645 mV.[1] The differences are generally attributed to hydrogen bonding and electrostatic effects from the surrounding protein and solvent.[2−5] Recent ligand K-edge X-ray absorption spectroscopy (XAS) experiments find large differences in the Fe−S covalency between HiPIPs and Fds apparently due to hydration[6] and attribute the redox potential differences to electronic effects of water hydrogen bonds based on a correlation between electrochemical redox potentials and metal−ligand bond covalencies in iron−sulfur complexes.[7] However, our combined density functional theory (DFT) and photoelectron spectroscopy (PES) studies indicate hydrogen bond effects are actually primarily electrostatic since the electronic structure and bonding of the clusters are not significantly affected.[8] Here, we present a new mechanism for redox tuning, namely the ligand conformation, which reconciles the seemingly conflicting experimental results.

Due to the complexity of the protein environment, the effects of hydration and ligand conformation on Fe−S covalencies and redox properties are separated using broken symmetry DFT (BS-DFT)[9] calculations of the analogue $[Fe_4S_4(SEt)_4]^{2-}$ (Et = ethyl), which is a good model for the $[Fe_4S_4(Cys)_4]^{n-}$ found in proteins.[8] Redox energies in the gas phase were calculated at the B3LYP/6-31(++)$_S$G**//B3LYP/6-31G** level, and Fe−L covalencies as measured by the percent ligand (%L) character mixing in the Fe 3d orbitals were obtained from natural bond orbital (NBO) analysis[10] of geometries at the B3LYP/6-31G** level. Thus, the calculations focus on a single effect at a time without approximations for the environment and take advantage of our previous calibrations of a variety of clusters against experiment.[11,12] Moreover, using these methods, vertical detachment energies (VDEs) correlate well with total %L character for a series of $[Fe_4S_4L_4]^{2-}$ clusters in the gas phase with different ligands,[12] in agreement with the above-mentioned XAS experiments.[6,7] However, the vertical reduction energies (VREs), which are defined similarly to the VDEs as the energy to add an electron without allowing relaxation, have a more complicated dependence on the total %L character.

To elucidate hydration effects, $[Fe_4S_4(SEt)_4]^{2-}$ was compared to hydrated complexes in which a water molecule was placed near each terminal or bridging sulfur ($[Fe_4S_4(SEt)_4]^{2-}$-HB(t) and $[Fe_4S_4(SEt)_4]^{2-}$-HB(b), respectively), resulting in a total of four water molecules per cluster. In the optimized structures, each water forms two hydrogen bonds, with $[Fe_4S_4(SEt)_4]^{2-}$-HB(t) slightly more favorable by ∼0.9 eV. Although VDE and VRE change by ∼0.7 eV upon hydration, the change in %L character is small and accounts for less than ∼0.1 eV of the VDE and VRE differences based on the correlation for other ligands (Figure 1). Thus, the major contribution to the redox potential differences appears to be the electrostatic

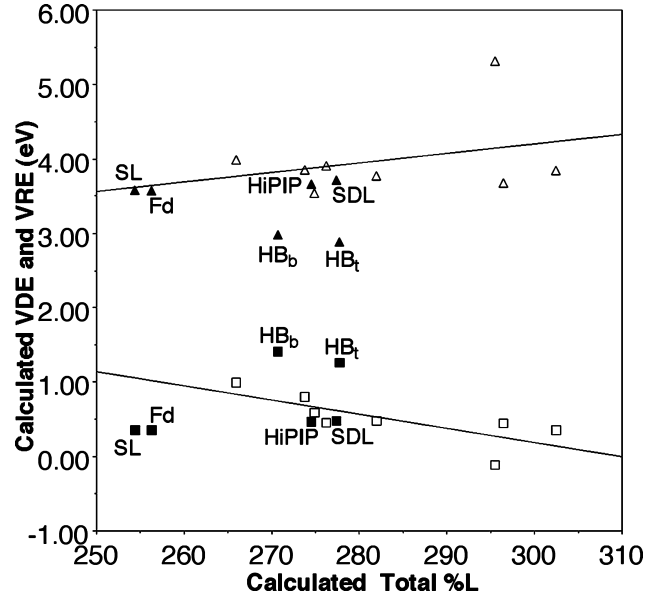

Figure 1. Correlation of the calculated total Fe−S/L covalency (%L) with VDE (□) and VRE (△) of $[Fe_4S_4L_4]^{2-}$ (left to right, L = Cl, SH, *S-tert*-butyl, SCH_3, $SeCH_3$, H, PH_2, and $P(CH_3)_2$ and with VDE (■) and VRE (▲) of $[Fe_4S_4(SEt)_4]^{2-}$ for the spin-delocalized state (SDL), the spin-localized state (SL), with waters hydrogen bonded to the bridging (HB_b) and terminal (HB_t) sulfurs, and in the Fd- and HiPIP-like conformations.

effect of the hydrogen bonds, consistent with PES/DFT studies[8] and protein calculations.[13−15]

However, the %L character of the HiPIPs and the Fd are significantly different in the XAS studies, which must have an underlying cause. A possibility is suggested by another conformation of $[Fe_4S_4(SEt)_4]^{2-}$ with different χ_3 (C−S_t−Fe−S_b, where S_b is the bridging sulfur on the opposite layer and S_t is the terminal sulfur ligand) torsions (Figure 2) that has very similar VDEs and VREs but only 92% of the calculated total %L character of $[Fe_4S_4(SEt)_4]^{2-}$ (Figure 1), apparently due to the minority spin exchange states of the two antiferromagnetically coupled layers that comprise the cubane.[9] Specifically, $[Fe_4S_4(SEt)_4]^{2-}$, which is like the experimental conformational structure,[15] has all four $\chi_3 \approx 50°$ and the layers each have a minority spin delocalized to create a symmetric $Fe^{2.5+}$−$Fe^{2.5+}$ pair. On the other hand, the other conformer is characterized by two $\chi_3 \approx 85°$ and two $\chi_3 \approx 60°$ and has one layer in which the minority spin becomes localized to create an Fe^{3+}−Fe^{2+} pair, henceforth referred to as $[Fe_4S_4(SEt)_4]^{2-}$−SL (Figure 2). Similar spin states have been found in the fission transition state of [4Fe−4S] clusters[16] and in the heteroligand $[Fe_4S_4(SCH_3)_2L_2]^{2-}$ (L = Cl, H).[17]

Two more conformations of $[Fe_4S_4(SEt)_4]^{2-}$ (Figure 3) were optimized from X-ray structures of redox sites of *Thermochromatium tepidum* (Tt)[18] HiPIP at 0.80 Å resolution ($[Fe_4S_4(SEt)_4]^{2-}$-

10.1021/ja900406j CCC: $40.75

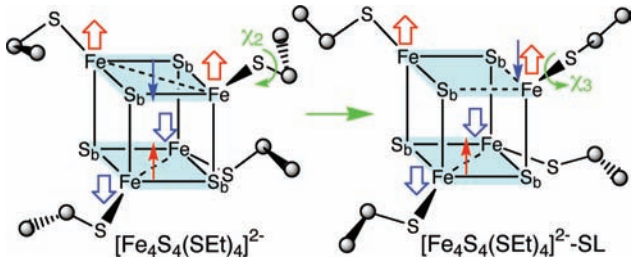

Figure 2. Schematic spin-delocalized $[Fe_4S_4(SEt)_4]^{2-}$ and spin-localized $[Fe_4S_4(SEt)_4]^{2-}$-SL structures.

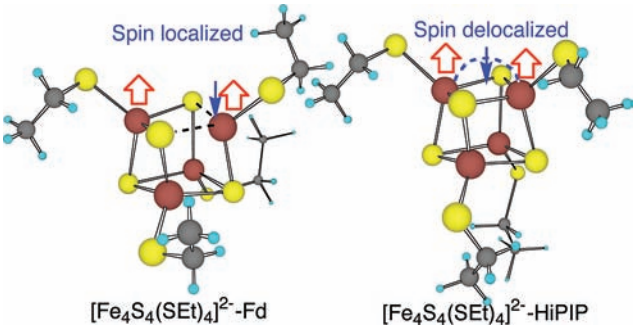

Figure 3. Calculated Fd- and HiPIP-like $[Fe_4S_4(SEt)_4]^{2-}$ structures.

HiPIP) and *Bacillus thermoproteolyticus* (Bt)[19] Fd at 0.92 Å resolution ($[Fe_4S_4(SEt)_4]^{2-}$-Fd). Interestingly, $[Fe_4S_4(SEt)_4]^{2-}$-HiPIP has two $Fe^{2.5+}-Fe^{2.5+}$ layers with $\chi_3 = -65°$ and $+68°$ for one and $\chi_3 = -153°$ and $172°$ for the other, and its cubane structure, spin state, and redox properties are similar to those of $[Fe_4S_4(SEt)_4]^{2-}$, in very good agreement with Mössbauer results of analogues and HiPIPs.[20] On the other hand, $[Fe_4S_4(SEt)_4]^{2-}$-Fd has one $Fe^{3+}-Fe^{2+}$ layer with $\chi_3 \approx 84°$ and $74°$ and one $Fe^{2.5+}-Fe^{2.5+}$ layer with $\chi_3 \approx -76°$ and $+66°$, and its cubane structure, spin state, and redox properties are similar to those of $[Fe_4S_4(SEt)_4]^{2-}$-SL. The $Fe^{2.5+}$ in Fd versus the Fe^{3+} in HiPIP also appears consistent with Mössbauer results in which the $[Fe_4S_4(Cys)_4]^{2-}$ cluster in Fd has less quadrupole splitting (ΔE_Q) than in HiPIP.[20,21] Remarkably, the calculated total Fe−S covalencies of $[Fe_4S_4(SEt)_4]^{2-}$-Fd and $[Fe_4S_4(SEt)_4]^{2-}$-HiPIP are 92% and 99% of $[Fe_4S_4(SEt)_4]^{2-}$ values, respectively, in good agreement with the experimental results that *Bt* Fd and *Chromatium vinosum* HiPIP are 85% and 96% of $[Fe_4S_4(SEt)_4]^{2-}$.[6]

In summary, BS-B3LYP calculations show dramatic changes in redox energies of $[Fe_4S_4(SEt)_4]^{2-}$ due to hydration with only slight changes in the Fe−S covalency. On the other hand, the conformational changes in thiolate ligands of $[Fe_4S_4(SEt)_4]^{2-}$-SL and $[Fe_4S_4(SEt)_4]^{2-}$-Fd induce minority spin localization, leading to large decreases in Fe−S covalency with only small changes in redox energies relative to $[Fe_4S_4(SEt)_4]^{2-}$ and $[Fe_4S_4(SEt)_4]^{2-}$-HiPIP. These findings suggest that the large change in the Fe−S covalency between Fd and HiPIP observed by XAS is due to differences in the conformations of the cysteinyl ligands of the cluster. Furthermore, the resulting differences in redox energies of ∼100 mV are significant; thus, ligand conformation is important to consider in understanding redox properties of iron−sulfur proteins.

Acknowledgment. This work was supported by a grant from the National Institutes of Health (GM-45303). The calculations were performed at the Environmental Molecular Sciences Laboratory, a national user facility sponsored by the U.S. DOE's Office of Biological and Environmental Research and located at Pacific Northwest National Laboratory, operated for DOE by Battelle, under Grants GC3565 and GC20901. Additional computational resources were provided by the William G. McGowan Foundation.

Supporting Information Available: The hydrogen bonding of terminal and bridging ligands of $[Fe_4S_4(SEt)_4]^{2-}$, $[Fe_4S_4(SEt)_4]^{2-}$-HB(t) and $[Fe_4S_4(SEt)_4]^{2-}$-HB(b) (Figure S1), the B3LYP/6-31G** optimized geometry parameters of spin-delocalized, spin-localized, Fd-like and HiPIP-like $[Fe_4S_4(SEt)_4]^{2-}$ structures (Table S1). These materials are available free of charge via the Internet at http://pubs.acs.org.

References

(1) Cammack, R. *Adv. Inorg. Chem.* **1992**, *38*, 281.
(2) Stephens, P. J.; Jollie, D. R.; Warshel, A. *Chem. Rev.* **1996**, *96*, 2491.
(3) Capozzi, F.; Ciurli, S.; Luchinat, C. *Metal Sites in Proteins and Models* **1998**, *90*, 127.
(4) Adman, E. T.; Watenpaugh, K. D.; Jensen, L. H. *Proc. Natl. Acad. Sci. U.S.A.* **1975**, *72*, 4854.
(5) Backes, G.; Mino, Y.; Loehr, T. M.; Meyer, T. E.; Cusanovich, M. A.; Sweeny, W. V.; Adman, E. T.; Sanders-Loehr, J. *J. Am. Chem. Soc.* **1991**, *113*, 2055.
(6) Dey, A.; Francis, E. J.; Adams, M. W. W.; Babini, E.; Takahashi, Y.; Fukuyama, K.; Hodgson, K. O.; Hedman, B.; Solomon, E. I. *Science* **2007**, *318*, 1464.
(7) Solomon, E. I.; Hedman, B.; Hodgson, K. O.; Dey, A.; Szilagyi, R. K. *Coord. Chem. Rev.* **2005**, *249*, 97.
(8) Yang, X.; Niu, S.; Ichiye, T.; Wang, L.-S. *J. Am. Chem. Soc.* **2004**, *126*, 15790.
(9) Noodleman, L.; Peng, C. Y.; Case, D. A.; Mouesca, J. M. *Coord. Chem. Rev.* **1995**, *144*, 199.
(10) All calculations were performed using the NWChem program package: Straatsma, T. P. et al. *NWChem, A Computational Chemistry Package for Parallel Computers*, version 4.6'; Pacific Northwest National Laboratory, Richland, Washington 99352-0999, USA, 2004.
(11) Wang, X.-B.; Niu, S.-Q.; Yang, X.; Ibrahim, S. K.; Pickett, C. J.; Ichiye, T.; Wang, L.-S. *J. Am. Chem. Soc.* **2003**, *125*, 14072.
(12) Niu, S.-Q.; Ichiye, T. *J. Phys. Chem. A* **2009**, *113*, in press.
(13) Jensen, G. M.; Warshel, A.; Stephens, P. *J. Biochem.* **1994**, *33*, 10911.
(14) Beck, B. W.; Xie, Q.; Ichiye, T *Biophys. J.* **2001**, *81*, 601.
(15) Hagen, K. S.; Watson, A. D.; Holm, R. H. *Inorg. Chem.* **1984**, *23*, 2984.
(16) Niu, S.-Q.; Wang, X.-B.; Yang, X.; Wang, L.-S.; Ichiye, T. *J. Phys. Chem. A* **2004**, *108*, 6750.
(17) Niu, S.-Q.; Ichiye, T. *J. Phys. Chem. A* **2009**, *113*, in press.
(18) Liu, L. J.; Nogi, T.; Kobayashi, M.; Nozawa, T.; Miki, K. *Acta Crystallogr., Sect. D* **2002**, *58*, 1085.
(19) Fukuyama, K.; Okada, T.; Kakuta, Y.; Takahashi, Y. *J. Mol. Biol.* **2002**, *315*, 1155.
(20) Beinert, H.; Kennedy, M. C.; Stout, C. D. *Chem. Rev.* **1996**, *96*, 2335.
(21) Mouesca, J. M.; Lamotte, B. *Coord. Chem. Rev.* **1998**, *180*, 1573.

JA900406J